Large parallel cosmic string simulations: New results on loop production

Jose J. Blanco-Pillado, Ken D. Olum, and Benjamin Shlaer

Phys. Rev. D **83**, 083514 — Published 15 April 2011

DOI: 10.1103/PhysRevD.83.083514

Large parallel cosmic string simulations: New results on loop production

Jose J. Blanco-Pillado, Ken D. Olum, and Benjamin Shlaer

Institute of Cosmology, Department of Physics and Astronomy, Tufts University, Medford, MA 02155, USA

Abstract

Using a new parallel computing technique, we have run the largest cosmic string simulations ever performed. Our results confirm the existence of a long transient period where a non-scaling distribution of small loops is produced at lengths depending on the initial correlation scale. As time passes, this initial population gives way to the true scaling regime, where loops of size approximately equal to one-twentieth the horizon distance become a significant component. We observe similar behavior in matter and radiation eras, as well as in flat space. In the matter era, the scaling population of large loops becomes the dominant component; we expect this to eventually happen in the other eras as well.

I. INTRODUCTION

The formation and evolution of field theoretic cosmic strings has been extensively studied for the past thirty years (See [1] and references therein). The idea [2] that superstrings could be stretched to cosmological scales by the expansion of the universe has recently [3–5] revived the interest in cosmic string networks. The existence of a cosmological network of strings may yield observational signatures that can be detected with current or planned experiments, giving us the opportunity to probe new physics at tremendous energy scales. This has motivated the study of many aspects of cosmic strings.

Early work on cosmic strings focused on the simple and generic observational predictions arising from their kinematic gravitational effects, namely searching for their imprint on the cosmic microwave background via the Kaiser-Stebbins effect [6], or by looking for the telltale identical pair of images of an astrophysical object being lensed by a cosmic string [7]. These effects are enhanced by increasing the energy scale of the string, and can therefore be used to place an upper bound on the dimensionless string tension $G\mu$ [8–10]. Another observational signature predicted by the evolution of a cosmic string network is the existence of a stochastic background of gravitational waves [11] emitted by the oscillating string loops which continually break off the network. This is an important effect since it allows the loops to shrink and decay, preventing them from becoming a dominant contribution to the energy budget of our observable universe. Particular features of the string evolution, such as cusps and kinks, create a focused burst rather than stochastic gravitational wave emission, and so allow much lighter strings to produce a detectable intermittent signal [12]. Additionally, cosmic strings can also produce other forms of radiation, either due to the partial annihilation of the string itself in regions of high curvature [13–16], or due to the their coupling to some other nongravitational degree of freedom such as an axion [17], a dilaton [18], or some other light field [19]. Radiation of this type has been studied in connection with cosmic ray physics, where we can use the observational bounds on these fluxes to place limits on the parameters of the cosmic string models [20].

However, it is clearly necessary to understand the statistical properties of the cosmic string network in detail before we can obtain robust predictions of observational signatures. Characterizing the essential properties of the network throughout its evolution has been approached in several different ways. Early work on this subject studied the properties of the network with analytical methods [21–23]. The central thesis of this work was the approach of the network to a *scaling solution* whereby the strings contribute a constant fraction of the energy density of the universe. The existence of a scaling solution is paramount to the viability of cosmic string models, since the network would otherwise become the dominant fraction of energy in the universe, in clear contradiction with observations.

After the initial impetus from the analytical description of the scaling solution, people turned to numerical simulation as a technique to compute the relevant parameters of the string network. Several groups independently developed codes to evolve a network of Nambu-Goto equations in an expanding universe [24–28]. Perhaps the most interesting conclusion of all these papers was that there does exist a scaling regime for long ("infinite") strings, where the average distance between the strings, $d(t)$, and the coherence length, $\xi(t)$, both scale in proportion to the particle horizon distance, given by $d_h(t) = a\eta$, where η is the conformal time and a the scale factor.

$$d(t) \sim \xi(t) \sim d_h(t) \sim t. \tag{1}$$

In fact, although the codes were significantly different, they appeared to be close to a quantitative agreement on the parameters of the network.

Further analytical work has been done by several different groups [29–31], but the necessity of large numerical simulations in understanding the properties of the string network over a large range of scales has always remained. The constant improvement of computers and the introduction of new algorithms allowed for a second generation of numerical simulations [32–36] of much larger size. Ref. [33] studied the loop number density and loop energy distribution and found an approach to scaling values of these quantities for loop sizes above a few thousands of the horizon size. Then Refs. [35, 36] studied the loop production function and found an approach to scaling in that function, but their results were not compatible with the loop distribution found by [33].

Refs. [9, 10, 14] simulated cosmic string loop networks using lattice field theory, but their results did not agree with the Nambu-Goto simulations of other groups. Instead, they found very significant emission directly from long strings. Attempts by other groups to reproduce this effect in field theory simulations [15, 16] did not succeed.

One of the realizations which emerged from all these efforts was that there are two different time scales associated with the approach of a network to scaling. The first time scale parametrizes the way long strings in the network reach a steady state with the correct macroscopic properties of the scaling solution, and a second, much longer time scale is associated with the small scale structure of the network. In other words, the component of the network produced in loops, as well as the short wavelength spectrum of perturbations on long strings seem to approach scaling at a slower rate. This makes their study much more difficult in numerical simulations, where one is limited by computational resources. This has motivated us to develop a code based on new parallel simulation techniques [37] which allows us to run simulations with dynamic range an order of magnitude larger than those previously reported in the literature. The results of these simulations will be described in a series of papers. Here we focus on the loop production function.

With a larger dynamic range, it becomes possible to clearly distinguish behavior at two relevant length scales, namely the "smallest scales" (i.e., the simulation resolution, the gravitational backreaction scale, or in our case the scale of initial conditions), and the scale set by the particle horizon. There is an ongoing controversy as to which scale is important in determining the typical size at which loops are produced. Roughly speaking, the claims are that all loops are produced at scales set by the particle horizon [21, 22], that all loops are produced at the smallest scales [26–28], or that some mixture of both are produced [31, 38].

Our results confirm those of Olum and Vanchurin [36], and our new techniques enable us to study loop production in much more detail and to much later times. We see a significant fraction of loop production in a broad, scaling peak reaching downward from about one twentieth of the horizon scale, along with an initially dominant but decreasing population at the smallest scales. This is true in both the matter and radiation eras, as well as in flat space. In the matter era, the horizon-scale population becomes dominant at late times. We expect this to happen as well in the radiation and flat-space cases, but we are not currently able to run long enough simulations to see whether such regimes develop. There appear to be two different peaks in the scaling spectrum of loops at significant fractions of the horizon size.

II. SIMULATION TECHNIQUES

The first step of any cosmic string simulation is to establish the initial distribution of strings. We have used the procedure of Vachaspati and Vilenkin [39] to generate the initial configuration of the network. This procedure constructs a string from the square faces that it must pass through. For each such face, we choose a random position on that face equally distributed in a square filling the central 20% of the face in each direction, and we connect each position to the next by a straight string segment. For each such segment, we then choose a velocity v in a random direction perpendicular to the string with v^2 evenly distributed between 0 and 0.25. These random perturbations mitigate the lattice nature of the initial conditions.

The algorithm for the subsequent evolution of Nambu-Goto strings is based on that presented in [32], where the strings are described by a collection of straight segments linked together to form kinky long strings and loops. These piecewise linear strings can be simulated exactly (up to computational arithmetic error) in flat space [32]. In an expanding background one can write the equations of motion for the string in conformal coordinates so that the causal structure of Minkowski space is preserved. The resulting equations cannot be analytically solved, but they can be well approximated by expanding the solution to first order in the product of H, the expansion rate of the universe, and the segment size being simulated [36]. This approximation improves as the simulation progresses since the Hubble distance grows relative to the size of the segments.

The other important ingredient in this algorithm is the intercommutation of string when two pieces of the string worldsheet intersect. It is believed that most gauge theory cosmic strings would intercommute with a probability P of essentially unity. But this may not be true for fundamental strings in a 4-dimensional compactification, where the probability of such a process is suppressed. In the present paper we will only explore the case $P = 1$. Other cases will be studied in subsequent publications.

The evolution of the string network continually produces loops of all sizes. It is useful to distinguish between the sub-horizon "loops" and the super-horizon "long strings" which make up the rest of the network. In our periodic space, all simulated strings are technically loops, and so we classify them by defining loops to be those strings which will never intersect any other string, including themselves. Due to the nature of our evolution algorithm it would be computationally intractable to evolve tiny loops, so we must remove them at some point. Loops whose physical size is much smaller than the interstring distance are likely to evolve without intersecting with any other string. In flat space we expect small loops to fragment until eventually all the string energy in the loop ends up in non-self-intersecting trajectories. It is then safe to log and remove those loops from the simulation, since they would not have any effect on the network properties. In an expanding universe the situation is complicated by the fact that loops are affected by the cosmological friction, so a non-self-intersecting loop could, in principle, be destabilized and chop itself up, triggering a new stage of fragmentation. We expect this effect to be negligible for any loop of size significantly smaller than the Hubble distance. We have checked that this is not an important effect by letting non-self-intersecting loops oscillate a number of times before being removed. The results do not show any significant deviation in any of these cases.

One of the main goals of this project is to extend the dynamic range of prior simulations performed using similar algorithms. Due to the fact that the simulations exist in a periodic space, the dynamic range is limited by the time it takes information to propagate across

the box. A possible solution to this problem was implemented in [32, 35] by periodically doubling the size of the box of the simulation. Here we have chosen an alternative way to extend the running time, by splitting the box into different regions that are simulated by many different computers, in other words using a parallel code. This allows us to faithfully simulate cosmic strings in a much bigger box, and consequently to run to much later times. We developed, to this end, a parallel Nambu-Goto string simulation using the algorithm of [32, 35, 36] and reported on preliminary results in [40]. This parallel method proved to be indeed superior to the single processor codes, but it also had some inefficiencies associated with the very different work loads that different processors encounter in a simulation of this kind. At late times, some regions of the simulation volume will have little or no string, while others will have a great deal. In such a case, the power of parallel computing is greatly diminished, since all the other processors must wait for the one with the most simulation work to do. Faced with that difficulty we have developed a new parallelization technique, whereby the spacetime volume is divided into small 4-volumes whose boundaries are lightlike, i.e. they have only initial and final surfaces. This permits the individual 4-volumes to run independently of one another, imposing only that each individual job must wait for those who provide data for its initial surfaces. This new method is particularly useful for our type of simulation, and it has allowed us to increase the dynamic range by almost an order of magnitude with respect to all previous cosmic string simulations. A detailed account of this new technique and its comparison with conventional parallelization methods is given in [37].

Our technique naturally gives rise to a periodic simulation volume in the form of a rhombic dodecahedron with opposite faces identified. A point and its images form a face-centered cubic lattice. We will refer to the constant comoving distance between a point and its closest images as the size of the simulation volume, L. The comoving volume being simulated is thus $V = L^3/\sqrt{2}$. The face-centered cubic lattice is close-packed, so the ratio of V to L^3 is the smallest possible. As shown in [36], the rate of information propagation through the simulation volume is about half the speed of light, so in a box of size L, we can run a simulation whose duration in conformal time is also L.

We have run simulations in flat space of size 2000 for a conformal time duration[1] 2000 in units of the initial cell size of the Vachaspati-Vilenkin algorithm. Such a simulation contains at maximum about 14 billion linear pieces of string simultaneously, and in the course of evolution creates about 1 trillion segments and produces about 10 billion loops of string. If one counts the largest total amount of data existing at one moment of simulation time, we believe this ranks among the largest simulations of any kind ever performed.

In the expanding universe we are not able to simulate as large a volume. The reason is that as the universe expands, the comoving length of linear pieces of string decreases (i.e., they are not purely stretched with the expansion). Thus, while the density of string in expanding cases is not very different from the flat case at the same time, the number of pieces of string to be simulated is much larger, and so the simulation effort much greater.

In the case of the radiation era, this has limited us so far to simulations of size 1500. In the matter era, the expansion is much more rapid and the problem more severe; the largest simulations we have so far run had size 500.

Once one has decided to create strings with a Vachaspati-Vilenkin cell size of 1, one must choose a conformal time η_i for the start of the simulation. This time determines the horizon distance, which will be used to define scaling, and in the expanding universe it controls the Hubble constant, which determines the rate of redshifting and stretching. We choose η_i so

[1] We work throughout in units where the speed of light is 1.

that the initial conditions correspond as closely as possible to the conditions that one would expect (based on later stages in the simulation) in a scaling solution at that time.

In the matter era, we found the best initial conformal time to be 4.5. We can thus run until conformal time 504.5, without contamination from the periodicity of the volume. Our dynamic range, defined as the ratio of final to initial conformal time, is thus 112. In the radiation era, we chose initial time 6. We can thus run until conformal time 1506, for dynamic range 251. In flat space, we chose initial time 4.0 and ran until time 2004, for a dynamic range of 501.

These dynamic ranges are much larger than those of any previous simulation. The largest simulation before this was done by our group [36] and claimed dynamic range 60 in the matter era and 120 in the radiation era. However, that claim was based on an artificial setting of the initial clock to 2.0 and 1.0 respectively. The initial conditions in those simulations were more appropriate for initial times of order 4.5 and 6.0, giving effective dynamic ranges 27 and 20. Ref. [33] used dynamic range 8 in matter and 17 in radiation, and all other previous simulations were smaller. A snapshot of a flat-space simulation is shown in Fig. 1.

III. SCALING NETWORK DYNAMICS

Suppose that the cosmic string network does evolve into a scaling regime. Then we hope that simulations will show an approach to this regime. What should we look for?

A. String density

First, let us consider scaling of the long string energy density, which is the easiest to find. Let d denote the average interstring distance of long strings, defined by

$$d = \sqrt{\frac{\mu}{\rho_\infty}}, \tag{2}$$

where μ is the tension of the string and ρ_∞ is the energy density of the long string network. In a scaling regime we expect this distance to be proportional to the horizon distance $d_h = a\eta$, so that

$$\gamma = \frac{d}{d_h} \tag{3}$$

is a constant.

B. Loops

Now let us turn to the distribution of loops. We characterize loops by their energy μl, and we call l the length. Some groups have concentrated on the the loop density distribution, which we will denote here as[2]

$$n(l,t) = \frac{dN}{dl\, dV} \tag{4}$$

[2] But note that [35, 36] used $n(l,t)$ to denote the production density, which we call $f(l,t)$ here.

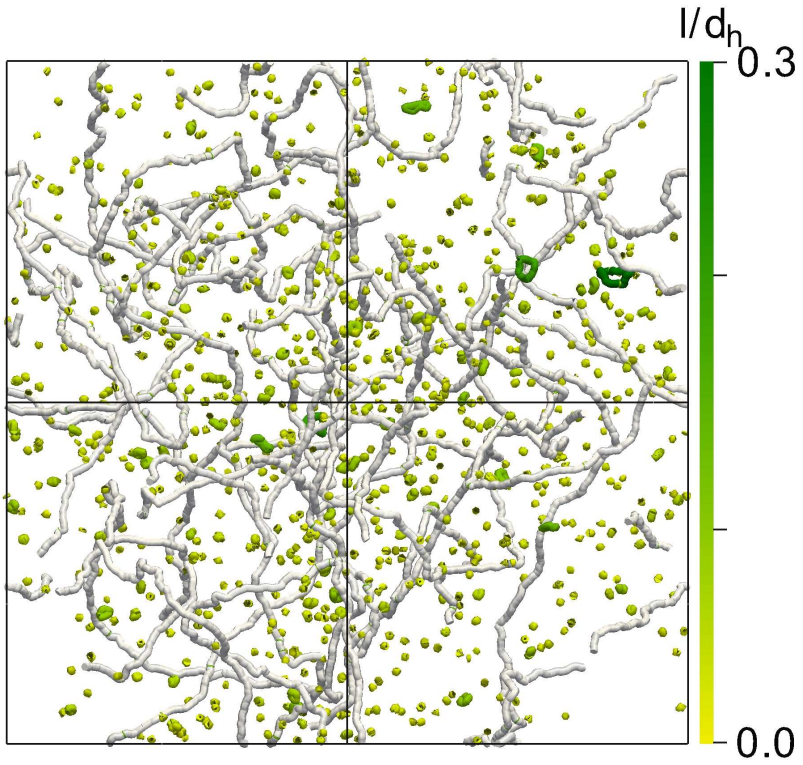

FIG. 1. (Color online) A picture of the string network at time 500 in a flat-space simulation of size 500. Long strings (here, any loop longer than the horizon size) are shown in light gray and loops are colored (shaded) according to their length, defined as total energy divided by μ. Non-self-intersecting loops smaller than length 10 have been removed. The edges of the simulation volume are shown as black straight lines. The rhombic dodecahedron is seen from one of the order-4 vertices, so that its projection looks square. The side of the square is the horizon distance, 500 units. The largest loop, shown in dark green (dark gray) on the far right above the centerline has length about 148. It appears much smaller because it is wrapped into a closed loop, because it has depth that cannot be seen, because it is wiggly, and because its length includes its kinetic energy. Loops of this size are rarely seen in the loop production function, so this loop will probably fragment or rejoin the long string network.

so that $n(l,t)dl$ is number of loops in the network at time t whose lengths lie between l and $l+dl$. Others concentrate on the density of loop production, which we will denote

$$f(l,t) = \frac{dN}{dt\,dl\,dV} \tag{5}$$

so that $f(l,t)\,dt\,dl$ is the number of loops produced per unit volume with $l \in [l, l+dl]$ at times $t \in [t, t+dt]$.

To put these functions in terms of scaling variables, we trade the loop length l for a length in scaling units, $x = l/d_h$. Similarly, we will use a scaling length interval dx and a scaling

spatial volume d_h^3 or spacetime volume d_h^4. Thus we define the dimensionless functions

$$n(x) = d_h^4 n(l,t) \tag{6}$$

and

$$f(x) = d_h^5 f(l,t). \tag{7}$$

We write the left-hand sides as functions of x, since in a scaling regime these functions will depend only on x, not on time.

C. Energy balance

The production of loops and scaling of long strings are related. If we consider a long piece of string whose length is l, the expansion of the universe will stretch and redshift it according to the relation [22]

$$\frac{dl}{dt} = Hl\left(1 - 2\left\langle v_\infty^2 \right\rangle\right) \tag{8}$$

where $\langle v_\infty^2 \rangle$ is the average squared velocity of the long strings. The energy density in long strings then obeys the Boltzmann equation

$$\frac{d\rho_\infty}{dt} = -2H\left(1 + \left\langle v_\infty^2 \right\rangle\right)\rho_\infty - \mu \int_0^\infty l f(l,t)\, dl. \tag{9}$$

Now consider a cosmology with scale factor $a \sim t^\nu$, so that ν is equal to 0 in flat spacetime, 1/2 for radiation domination, and 2/3 for matter domination. The horizon distance is then $t/(1-\nu)$. In a scaling regime $\rho_\infty = \mu/(\gamma^2 d_h^2)$, so we can rewrite Eq. (9) as

$$\int_0^\infty l f(l,t)\, dl = \frac{2}{\gamma^2 d_h^3}\left(1 - \frac{\nu}{1-\nu}\langle v_\infty^2 \rangle\right). \tag{10}$$

In scaling variables, Eq. (10) becomes

$$\int_0^\infty x f(x)\, dx = \frac{2}{\gamma^2}\left(1 - \frac{\nu}{1-\nu}\langle v_\infty^2 \rangle\right). \tag{11}$$

A consequence of Eq. (11) is that any scaling loop production function $f(x)$ must be normalizable, in the sense that the left-hand side of Eq. (11) converges.

Below, we will measure γ and $\langle v_\infty^2 \rangle$ in our simulations and use them to predict the left-hand side of Eq. (11), as a check on the consistency of our results.

D. Integrated loop production

The loop density distribution arises from all prior production of loops. We will ignore gravitational damping, which is not included in our simulation. We also, at first, ignore the decrease in the energy of loops from redshifting of their center-of-mass velocities. In this approximation, subhorizon loops retain their physical length l, and the only change in the distribution of loops in a comoving volume is due to the production of new loops from the long string network. Thus

$$\frac{d}{dt}\left[a^3(t)n(l,t)\right] = a^3(t)f(l,t). \tag{12}$$

Accordingly we can find $n(l,t)$ from $f(l,t)$ by integration,

$$n(l,t) = \frac{1}{a^3(t)}\int_0^t a^3(t')f(l,t')\,dt' = \int_0^t \left(\frac{t'}{t}\right)^{3\nu} f(l,t')\,dt', \tag{13}$$

since $a(t) \sim t^\nu$.

We would like to write this in terms of the scaling functions $n(x) = d_h^4(t)n(l,t)$ and $f(x) = d_h^5(t)f(l,t)$. Let us change the integration variable from t', the creation time of the loop, to $x' = l/d_h(t')$, the scaling length that it had when it formed. We similarly exchange t'/t for x/x' to get

$$n(x) = (1-\nu)x^{3\nu-4}\int_x^\infty x'^{\,3-3\nu} f(x')\,dx'. \tag{14}$$

Since ν is at most $2/3$, $3-3\nu$ is at least 1. Since $f(x)$ must be normalizable (in the sense of Eq. (11)), the integral on the right hand side of Eq. (14) converges even if x is taken to 0. Thus for loops sufficiently below the horizon size ($x \ll 1$), Eq. (14) is insensitive to the lower limit, and we get a power-law prediction [1] for the loop density distribution,

$$n(x) = \omega_\nu x^{3\nu-4}, \tag{15}$$

with

$$\omega_\nu = (1-\nu)\int_0^\infty x^{3-3\nu} f(x)\,dx. \tag{16}$$

Now let us consider the effect of the center-of-mass velocity of emitted loops on Eq. (14). We will continue to neglect gravitational damping. As we will show below, typical loop velocities increase with decreasing x, and tiny loops are usually emitted with quite large boosts. For simplicity, we will assume that the dominant contribution to Eq. (14) comes from a single x_1 corresponding to a typical loop center-of-mass velocity v_1. For x near x_1, the effects are somewhat complicated [41], and we will not attempt to model them here, but for $x \ll x_1$ matters are simpler. In this case, the most important loops have been redshifted essentially to rest, and thus their energy has decreased by a factor $\gamma_1 = (1-v_1^2)^{-1/2}$.

Thus we can update our calculation by taking loops with length l to have been formed with length $l' = \gamma_1 l$. Equation (13) becomes

$$n(l,t) = \gamma_1 \int_0^t \frac{t'^{\,3\nu}}{t^{3\nu}} f(l',t')\,dt'. \tag{17}$$

The factor of γ_1 arises because $n(l,t)$ is the loop density per unit l, while $f(l',t')$ is the loop production density per unit l' and $dl'/dl = \gamma_1$.

The relationship between x' and t' is now $x' = l'/d_h(t') = \gamma_1 l/d_h(t')$ so $x/x' = t'/(\gamma_1 t)$, and we find once again that for $x \ll x_1$ we have Eq. (15), but with

$$\omega_\nu = (1-\nu)\gamma_1^{3\nu-3}\int_0^\infty x^{3-3\nu} f(x)\,dx. \tag{18}$$

Equation (15) tells us that the scaling loop density distribution $n(x)$ has a universal form (for small x) that does not depend on the shape of $f(x)$, except in an overall factor. The

only way that a simulation could find a function $n(l,t)$ whose $l \ll t$ behavior does not have the form $d_h^{-4} n(x)$ with $n(x)$ given by Eq. (15) is for the loop production in that simulation to not be in a scaling regime.

This conclusion applies even though real cosmic strings, unlike those in usual simulations, would be affected by gravitational damping. It does not make sense to claim that simulations indicate a nonnormalizable $f(x)$, but that $f(x)$ will be cut off for low x by gravitational damping. If simulations indicate a scaling function $f(x)$, then if one did a very long simulation, one should observe $f(x)$ approaching that scaling form. In order to approach a nonnormalizable $f(x)$, the fraction of the energy of the string network emitted into loops in a Hubble time in the simulation would have to grow without bound. Such a situation could never be found in a simulation that conserved energy, so such a result does not make sense.

The same argument applies to analytic claims about loop production functions. It is not reasonable to predict a nonnormalizable $f(x)$ on the basis of analytic reasoning that ignores gravitational back reaction, and then claim that such a thing is made acceptable by the inclusion of gravity. What could such analysis predict about strings with infinitesimal $G\mu$, so that gravity could be ignored? Some consistent answer should emerge, which means that the nonnormalizable growth of $f(x)$ would have to be cut off at some small x. One must then analyze whether this cutoff is at a smaller or larger scale than that produced by gravitational damping, which would depend on the value of $G\mu$ under consideration.

IV. RESULTS: LONG STRING DENSITY

We now present results from our simulations, beginning with the scaling of the long string density. Long strings are commonly defined as those whose energy is above some threshold. Here, however, we distinguish the long strings from the loops based on interactions. If a loop undergoes 3 oscillations[3] without intersecting itself or another string, we retroactively consider it to be a loop beginning at the time when it was formed. Everything else belongs to the long string network.

With this definition, we compute the parameter $\gamma = d/d_h$, with d given by Eq. (2). For a scaling network we expect γ to achieve a constant value. In Fig. 2

we plot γ as a function of conformal time η. The top group of lines shows 13 runs of size 500 in the matter era, the middle group 6 runs of size 1500 in the radiation era, and the bottom group 4 runs of size 2000 in flat spacetime. In all cases, the scaling of long strings is well established early in the simulation. We note that in the flat case, the scaling results entirely from loop production, as there is no Hubble friction present.

Nevertheless, as seen in this plot against logarithmic time, the interstring distance is slowly changing, even at end of the simulations, so the final value cannot be precisely determined. At late times, there is also quite a lot of noise because of fluctuations in the actual long loops produced.

We average the interstring distance over all runs in each era at the end of the simulation, and show the results in Table I,

in comparison with previous simulations. In general we see good agreement with other recent results. The exception is the field theory simulations [10] which do not seem to agree with any Nambu-Goto simulation, and the flat space simulations of Ref. [34], which gave an interstring distance twice as large as ours.

[3] This is the minimum number of oscillations before our algorithm can confirm that the trajectory is non-self-intersecting. Changing this to a larger number does not significantly affect the results.

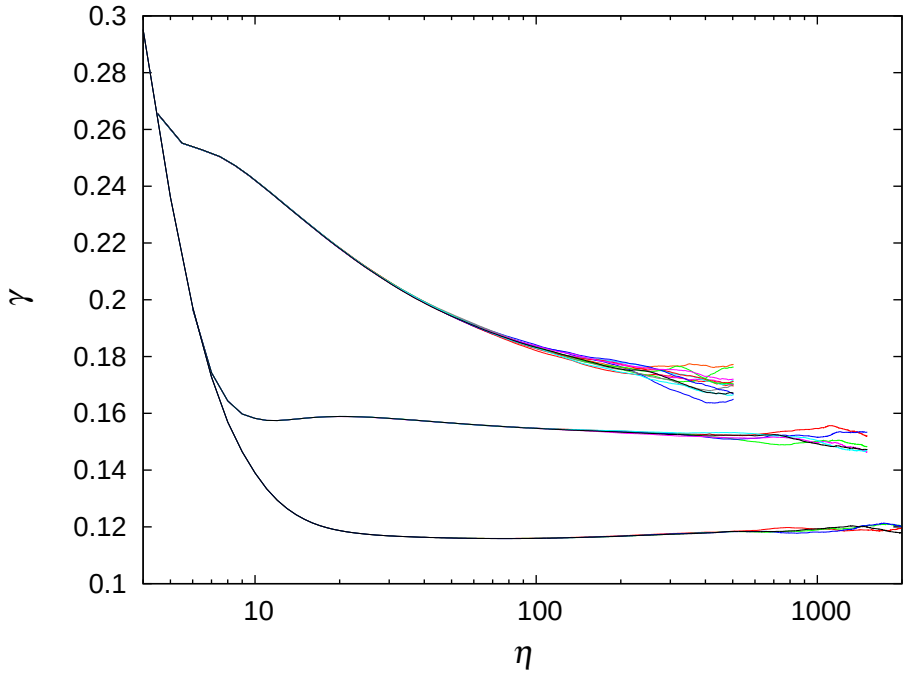

FIG. 2. The ratio of the interstring distance to the horizon size. The top group of lines is for the matter era, the middle group the radiation era, and the bottom group flat spacetime.

First author & Ref.	Flat	Radiation	Matter
Albrecht [25]		0.07	0.12
Bennett [27]		0.14	0.18
Allen [28]		0.13	
Vanchurin [32]	0.096		
Ringeval [33]		0.162	0.188
Martins [34]	0.23	0.13	0.20
Bevis [10]		0.255	0.285
This paper	0.12	0.15	0.17

TABLE I. Values of γ, the ratio of the interstring distance to the horizon size, from present and past simulations. Ref. [10] used lattice field theory and included all string in ρ_∞. All other simulations used Nambu-Goto, and all but the present paper included loops larger than some scaling threshold in ρ_∞. Here we include all loops which will fragment (or rejoin) in ρ_∞. This is the correct definition for the calculation of energy conservation in §V D below. Including only loops larger than the horizon size would increase γ by no more than 3%.

The agreement with other simulations whose dynamic range was significantly smaller than ours supports the conclusion that the long string component of the network finds its way to a scaling solution on a relatively short time scale, even if the other properties of the network have not relaxed to their scaling solutions yet. We will comment on this effect again when we discuss the scaling of loops.

V. RESULTS: LOOP PRODUCTION

In this section we study the loop production function $f(x)$ and the loop distribution function $n(x)$, as defined above. We consider a loop to be produced when it first enters a non-intersecting trajectory. Loops that fragment or that rejoin the long string network are not counted.

The distribution $f(x)\,dx$ gives the spectrum of loop production, which is not necessarily integrable. Instead we seek the distribution of power going into loops $xf(x)\,dx$. Due to the wide range of loop sizes covered by our simulations, it is illuminating to plot this power density in logarithmic units: $x^2 f(x)\,d\ln x$. In order to interpret the area under the curves as the total power produced in loops, we plot $x^2 f(x)$ on linear-log axes in the figures below.

A. Matter era

We have performed thirteen simulations on a comoving box of 500 initial correlation lengths each, in a matter era background. The initial conformal time was set to $\eta_i = 4.5$, and we ran until $\eta_f = 504.5$. Following the algorithm described above, we removed the non self-intersecting loops from the simulation, keeping record of their size and time of production. Using this information, we can reconstruct the loop distribution $n(x)$ and the loop production function $f(x)$ as time progresses to determine if either approaches a scaling regime.

We first turn our attention to the loop production function. We plot in Fig. 3 the data for $f(x)$. The error bars show one standard deviation from the thirteen successive runs.

The form of the curves in Fig. 3 is similar to that of [36], but because our simulation is larger than that of [36] we can follow the evolution of $f(x)$ to much later times.

Notice these curves have a slightly increasing area toward later times. This suggests the interstring distance d began at a value larger than its scaling value, and the initially lower power going into loops allowed it to decrease toward the scaling value. This is confirmed in Fig. 2. Why didn't we choose our initial time so that the initial $\gamma = d/d_h$ was equal to the scaling value? The reason is that we found it more important to have the the height of the small loop production peak start out unchanging in time, so that we could be sure that the decrease at later times (shown in Fig. 3) was not an artifact of the initial conditions. One cannot make both choices simultaneously because the structures on strings in the initial conditions are not very close to the scaling regime.

We can get a better look at the relative shapes of the curves in Fig. 3 by normalizing each curve to unity. This is done in Fig. 4, which now gives the relative flow of power into loops of different sizes.

We see that the normalized $f(x)$ appears to converge more rapidly to a final scaling form.

We can identify three different peaks in the loop production. The first is sharply peaked at $x \approx 0.05$, the second is centered approximately an order of magnitude smaller in x, and is much wider. The third peak is clearly moving toward smaller x, representing the transient (non-scaling) population of loops seeded by the initial conditions. The non-scaling peak is decreasing in area relative to the scaling portion of the distribution, and is subdominant after a conformal time of order 100. At the farthest reach or our simulation, the non-scaling power represents of order 25% of the total loop power, and we expect it to continue to decline in larger simulations.

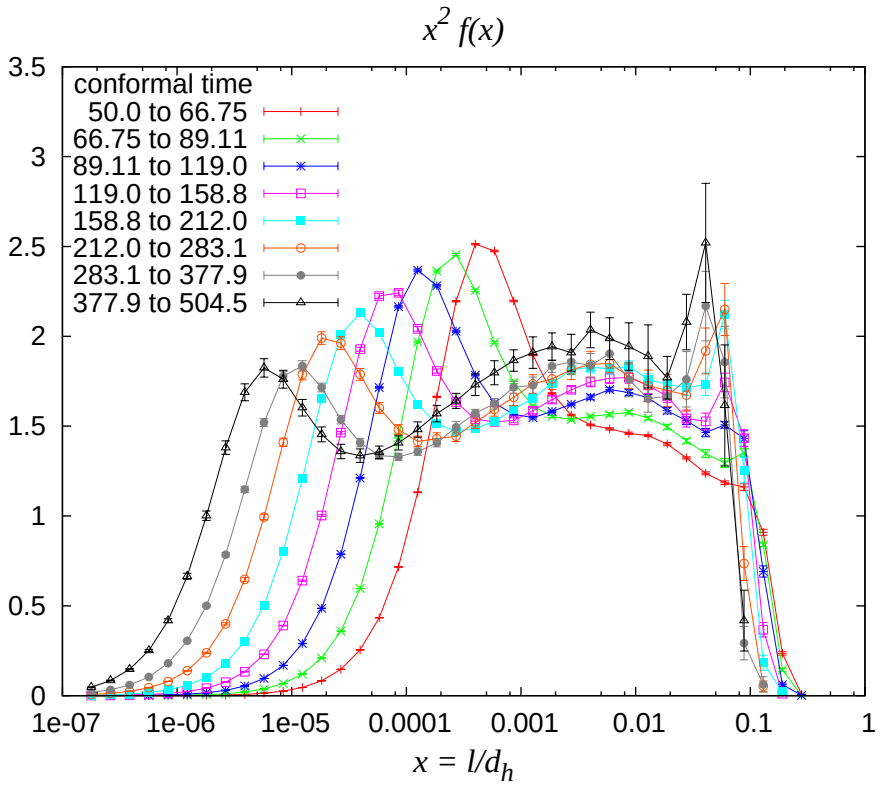

FIG. 3. (Color online) The spectrum of loop production power $x^2 f(x)$ in the matter era.

It is clear from the time dependence of $f(x)$ that the small scale structure and loop production has not completely reached scaling, but we consider the late-time behavior of our data to be evidence that a time-independent loop production function exists without the aid of an additional smoothing mechanism such as gravitational radiation. While it is possible that the non-scaling third peak will continue to evolve toward smaller x while maintaining a constant (but certainly subdominant) area, we do not expect this to be the case.

The other two peaks appear to scale: they do not move toward smaller x at later times. We do not know why there are two such peaks, but one speculation is that one peak represents loops which resulted by chance from two or more spacelike-separated intercommutations, while the other represents those that were formed from features on a long string by a single reconnection. Another possibility is that the peak with smaller x represents the results of fragmentation after loops are formed, while the peak with larger x represents those which happen to form in non-self-intersecting trajectories.

To study the center-of-mass velocities of loops, we define $p = v/\sqrt{1-v^2}$, the loop momentum per unit rest mass, and let $f(x,p)\,dx\,dp$ be the scaling production rate of loops with $x \in [x, x+dx]$ and $p \in [p, p+dp]$. To show $x f(x,p)\,dx\,dp$ we plot $x^2 p f(x,p)$ on logarithmic axes in Fig. 5. As expected, small loops at late times are mostly formed with ultrarelativistic speeds.

We now plot in Fig. 6 the number density distribution $n(x)\,dx$, which is represented by $x\,n(x)$ on logarithmic axes. We see that the solution is in good agreement with the results of Eq. (15), which for the matter era predict a power law behavior of the form x^{-1}. This

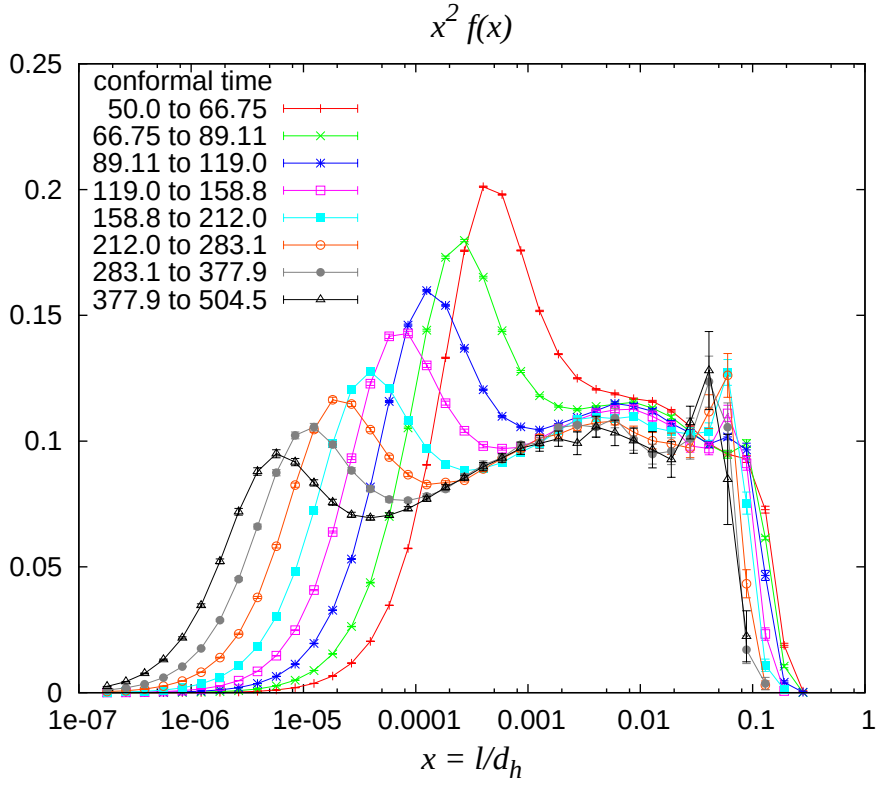

FIG. 4. (Color online) Normalized $x^2 f(x)$ during the matter era. While perhaps 70% of the power goes into initial-conditions loops at conformal time 50.0, less than 25% does so by conformal time 500.0.

is different from the result obtained in [33], where the power law was found to be of the form $x^{-1.4}$. As we showed in §III D above, the scaling form of $x\,n(x)$ could not go as $x^{-1.4}$ throughout the range of x where loops are produced. Either there must be significant loop production in the simulations of [33] at scales below where the $x^{-1.4}$ fit applies or their loop distribution must not have reached its final scaling form.

B. Radiation era

Fig. 7 shows less dramatic, but similar, scaling behavior in the radiation era, where we performed six simulations of size $L = 1500$ comoving initial correlation lengths. The results are again qualitatively similar to those of [36]. Notice that the total power going into loops is much higher for radiation domination than for matter.

The approach to loop scaling is much slower (in conformal time) than occurs in our simulations of the matter era. Nevertheless, it appears that a large but shrinking population of transient loops at the initial conditions scale is making way for a scaling population sharply peaked at $x = 0.05$, with a nearly flat distribution extending over many orders of magnitude, perhaps peaked an order of magnitude smaller in x.

We can understand the slower approach to scaling as follows. During radiation domination, the increase of scale factor with conformal time is much lower, and so strings are

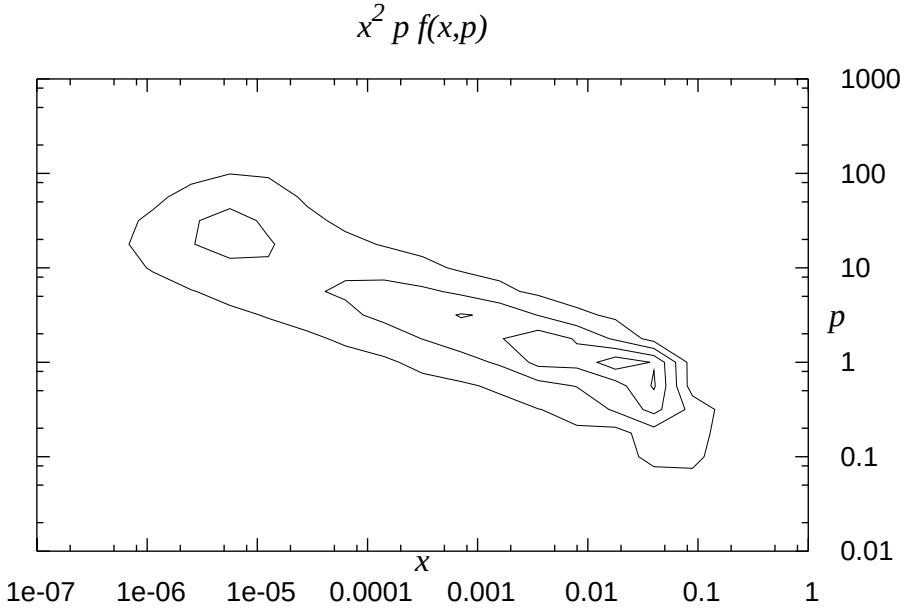

FIG. 5. Contour plot showing the distribution of loop power in the matter era, for conformal times from 283.1 to 504.5. Here $p = v/\sqrt{1-v^2}$.

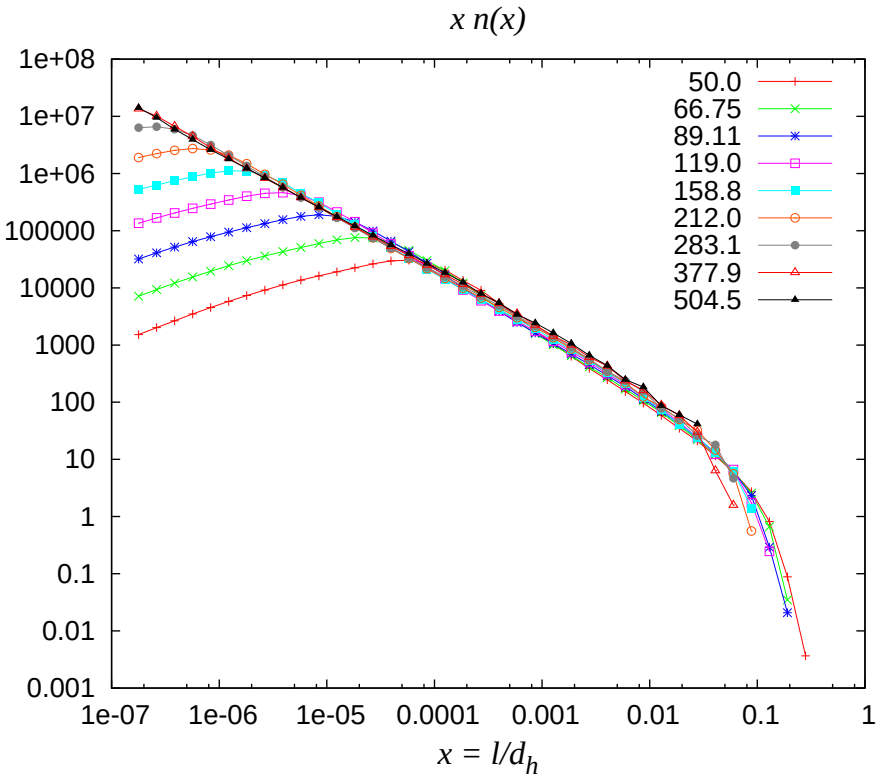

FIG. 6. (Color online) The number density distribution of loops $x\,n(x)$ during the matter era.

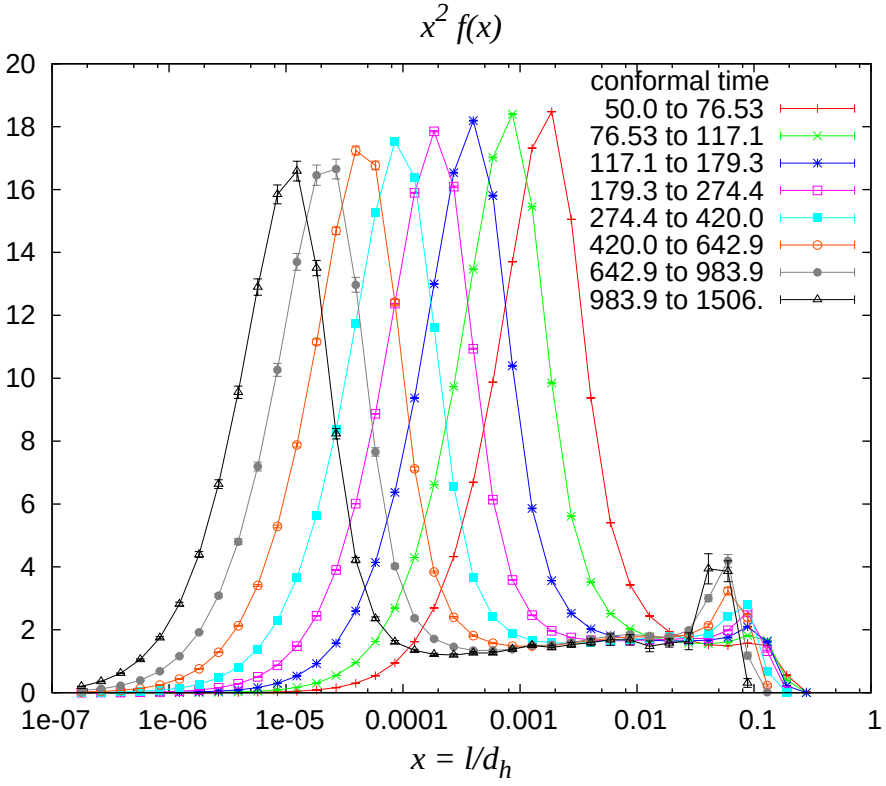

FIG. 7. (Color online) The loop production power $x^2 f(x)$ in the radiation era.

being stretched and thus smoothed more slowly, causing small-scale structure to persist for longer. Furthermore, the redshifting of string energy is less efficient than during the matter era, and therefore the network will need to make more use of loop production in order to reach a scaling solution, so the overall production rate is much higher.

We cannot predict the scaling form of $f(x)$ as well as we could for the matter era, since a dominant fraction of power is in the transient regime. But the late-time radiation era power looks similar to that in the matter era at a much earlier time. We expect that the radiation era evolution should be similar to that in the matter era, with the scaling features eventually dominating, and $f(x)$ eventually approaching a time-independent form, but the approach to scaling will last much longer.

The velocity dependence of the loop production function can be seen in Fig. 8.

We show in Fig. 9 our dataset $n(x)$ binned logarithmically from the simulation. The data obtained this way agrees quite well with the analytical results presented earlier for the radiation era, where $x\,n(x) = \omega_{\frac{1}{2}} x^{-3/2}$. This should not be misinterpreted as true scaling, since we know that a dominant portion of the power in loops is in a transient, not a scaling population.

Roughly speaking, there are three possibilities which can occur at very late times (assuming γ_r is static). The non-scaling peak could smear itself out as it continues to move toward smaller x while creating an extremely broad plateau. It could conceivably move off the plateau and continue indefinitely toward smaller x while maintaining a constant area. It could also decline while the peak at $x = 0.05$ grows, and not leave a tremendous plateau. We conjecture the last to be the case. It should be pointed out that the first two cases

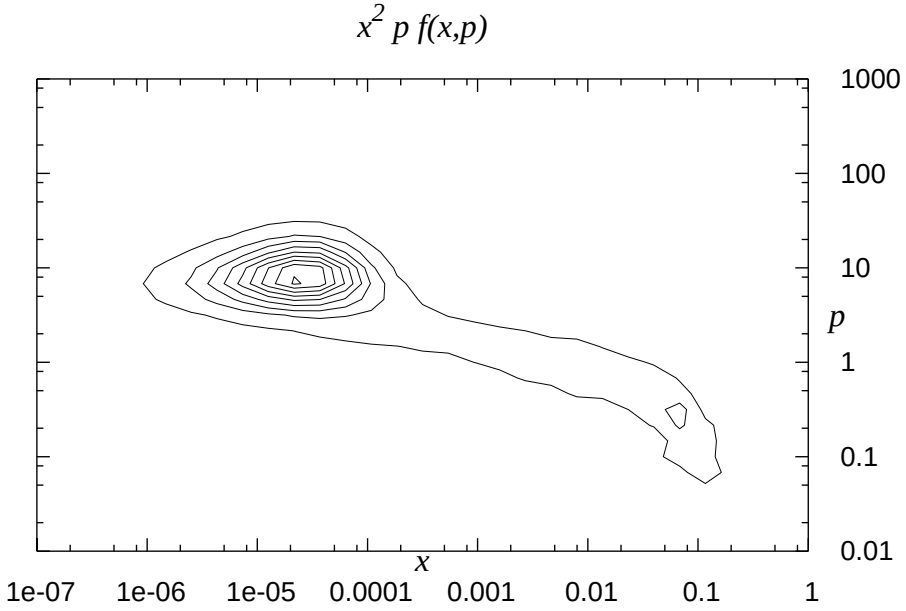

FIG. 8. Contour plot showing the distribution of loop power in the radiation era, for conformal times from 475 to 1006. Here $p = v/\sqrt{1-v^2}$.

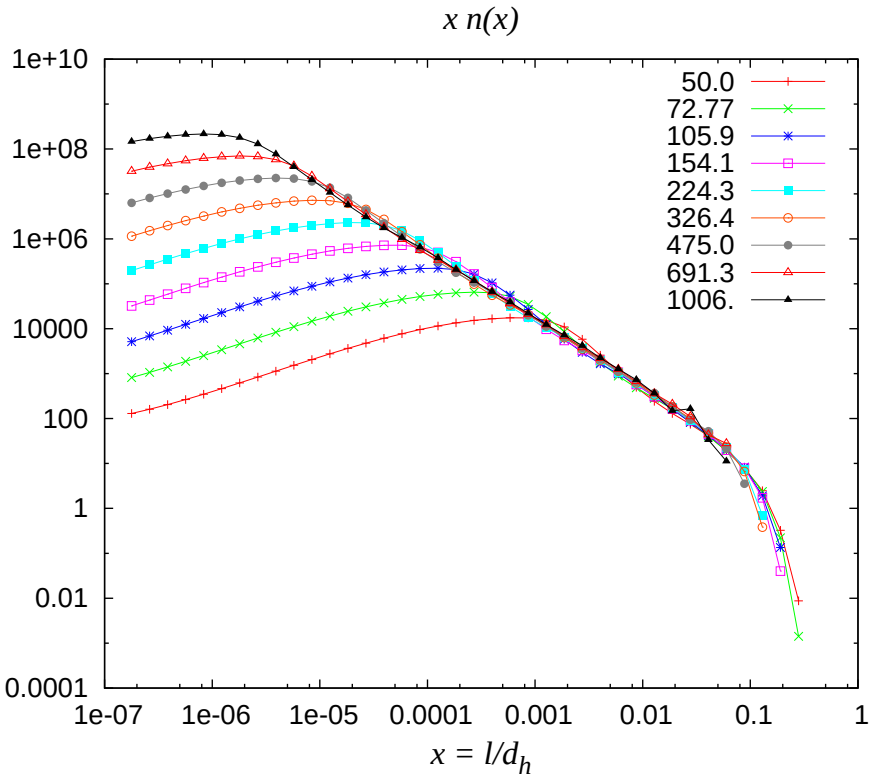

FIG. 9. (Color online) The number density distribution of loops $x\,n(x)$ during the radiation era.

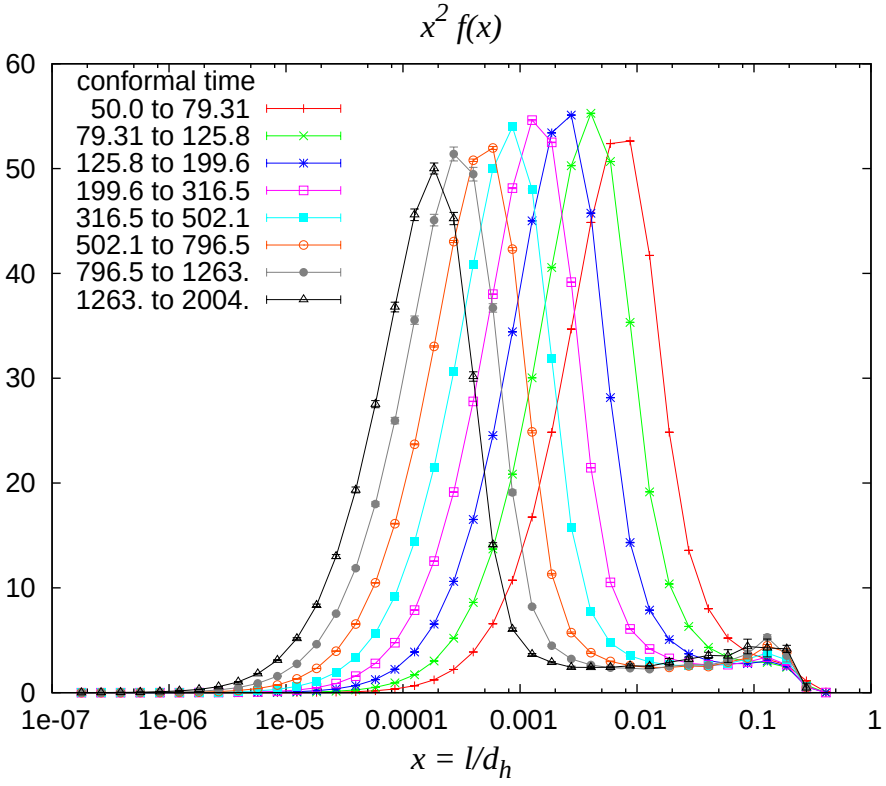

FIG. 10. (Color online) The loop production power $x^2 f(x)$ in flat spacetime.

are essentially identical in terms of the prediction for $\omega_{\frac{1}{2}}$, but that third case will cause a relative increase by up to an order of magnitude. It is this uncertainty which prevents us from claiming that the loop density shown in Fig. 9 is in the final scaling regime. This illustrates why the spectrum of loop power $f(x)$ is a more precise indicator of scaling than $n(x)$, the spectrum of existing loops.

C. Flat space

We present in Fig. 10 the results of our four simulations performed in a box of size 2000. Because redshifting is nonexistent, all smoothing of the strings comes from loop production. This massive loop production clearly smooths the strings enough for a scaling peak at $x \approx 0.1$ to appear, although it remains small even until conformal time 2000.

The results in Fig. 10 are qualitatively similar to those of [35], but the ratio of the scaling to the non-scaling peak height in [35] was significantly larger. There are several differences between the present simulation and that of [35], which make a direct comparison difficult. Ref. [35] achieved box size 800 by a technique of successive doublings of the box size [32], whereas we simulate a box of size 2000 directly. The box-doubling technique required intercommutation probability $P = 0.5$, whereas we use $P = 1$. We run only for an interval of conformal time equal to the box size L, whereas [35] ran significantly beyond conformal time 800. Finally, [35] used somewhat smoother initial conditions in which a point was interpolated between each pair of successive Vachaspati-Vilenkin faces, whereas we draw a

	γ	$\langle v_\infty^2 \rangle$	$\mathcal{P}_{\rm Prediction}$	$\mathcal{P}_{\rm Simulation}$
Matter	0.17	0.35	21	19
Radiation	0.15	0.40	53	51
Flat	0.12	0.45	139	136

TABLE II. Predictions from energy balance.

straight line between those points. Smoother initial conditions may have led to a lower peak at the initial-condition scale. Note also that [35, 36] show $x^2 f(x)$ on a logarithmic scale, whereas the vertical axis in Fig. 10 is linear.

Perhaps the most important features of Fig. 10 are the turnaround of the transient peak and the existence of a scaling peak. After a time $\eta \approx 150$, the amplitude of the transient peak begins to decrease. Following the arguments presented above, we again expect that this decrease will continue, leading to a loop production function consisting of a time-independent distribution peaked at $x \approx 0.1$.

D. Energy balance check

Having measured values for γ and $\langle v_\infty^2 \rangle$ directly from the simulations we can now use Eq. (11) to predict the total power emitted by the long string network in the form of loops, $\mathcal{P}_{\rm Prediction}$, and compare it with the direct computation of this power from the integral of the loop production function, namely,

$$\mathcal{P}_{\rm Simulation} = \int_0^\infty x f(x)\, dx. \tag{19}$$

We show in Table II the comparison of these quantities for the matter, radiation and flat eras. We see that the agreement between the predicted result and the numerically found value is within the statistical noise in all cases. We consider this is an important check for our simulations since it serves as a nontrivial test of our code and algorithms.

VI. CONCLUSIONS

We have developed a new parallel computing technique [37] that has allowed us to run the largest cosmic string simulations ever performed, reaching an increase in dynamic range of roughly an order of magnitude with respect to previous studies. The results of our simulations indicate a much slower approach to scaling for loops than for the long string contribution to the network. This clearly shows the need to push the dynamic range of the simulation to its largest possible extent in order to prevent contamination by transient states.

How is it possible for the interstring distance to be quite close to the final scaling value at early times, while the loop production function is still very far from scaling? Surely an important part (in flat space, the only part) of the loss of energy from the long string network is due to the production of loops, so if the loop production mechanism is not in a scaling regime, why does the energy loss rate scale?

The explanation is presumably that described by Bouchet [42]. The loops are produced by a two-step process. The first step is the intercommutation of infinite strings, which maintains

the interstring distance by the usual feedback mechanism in which an increase in the string network density leads to more intercommutations. The second step is the formation of loops triggered by or made up of the large kinks formed in the intercommutations. It controls how the removed string ends up in loops of different sizes. Thus the first step can be scaling long before the second.

Our simulations confirm the results of [35, 36]: There is an initially dominant transient feature in the loop production function which very slowly subsides to reveal a significant fraction of loops produced in a scaling regime. In the matter era, we find this population dominates over non-scaling loop production. Because this does not occur until extremely late times, we do not believe that prior claims of having found the final form of loop scaling in numerical simulations are correct.

In light of our results, we expect that the final loop production function will eventually be dominated by a broad peak of loop sizes proportional to the horizon size but ranging downward from about a twentieth of that size. We achieve this to good accuracy only in the matter era, where approximately 75% of loop power has achieved scaling by a conformal time of 500. This will clearly have an impact on the observational signatures of string networks. We will report on this in future publications.

ACKNOWLEDGMENTS

We would like to thank Vitaly Vanchurin and Alex Vilenkin for helpful conversations. This work was supported in part by the National Science Foundation under grant numbers 0855447 and 0903889. These simulations were performed using a total of 27 years of CPU time on the Tufts High-performance Computing Research Cluster. We are also grateful for access to the Nemo computing facility at the University of Wisconsin–Milwaukee. Nemo is funded in part by the National Science Foundation under grant 0923409.

Appendix A: Infinitely difficult cosmic string loops

We have identified some new features of Nambu-Goto cosmic strings which are impractical to faithfully simulate. One of these features can be called a "skipping stone." It occurs in particular cases when a network contains a loop which to good approximation is piecewise linear with five or six kinks, and which collides with a long straight segment of string. The collision may occur in such a way as to break off a loop again immediately afterward, one with less energy but precisely the same shape.

The problem is that the smaller loop will then repeat this process, skipping off the long string again and again, losing energy each time, but never changing shape. Just as a skipping stone leaves behind a geometric series of ripples, this loop will perform (in the Nambu-Goto approximation) an infinite number of intercommutations, leaving behind a geometric series of kinks on the string.

Such a physical process represents a nightmare for a numerical simulation which has no minimum resolution, since each of these ripples will be recorded and evolved.

To avoid the tremendous computational resources required to simulate these rare skipping stones all the way down to the minimum size set by the floating point resolution, we have intentionally failed to perform a certain, very small number of intercommutations. These avoided intercommutations are chosen to only include the collision of a disjoint loop with

another string, and so never prevent the formation of a loop. Furthermore, the avoided intercommutation must occur within a very short distance of a very large number of kinks, i.e., only after the stone has skipped at least 50 times do we allow it to pass through the surface of the water. The fraction of intercommutations we ignore is less than 0.2%.

Although these features occur with a varying degree of severity, and rarely plague small simulations, in a simulation of size 2000 they are virtually guaranteed to occur at least once with enough alignment so as to bog down one computer for literally days as it attempts to evolve through an amount of simulation 4-volume which normally takes a few seconds.

If cosmic strings exist, we expect that "infinite repetition" phenomena such as we discuss here occur in the real universe. Real cosmic strings would not have exactly straight segments, but this is of little consequence. If an approximation of the "skipping stone" phenomenon began, each successive iteration would involve shorter pieces of the original strings, which would thus be closer to straight. Of more importance is that the kinks separating the straight segments would not be infinitely sharp. Some kinks appear anew each cycle, but some remain from the original shape of the loop, and these would have been smoothed by gravitational back-reaction. Thus the gravitational damping scale would set a lower bound on the size of self-similar loops that could be produced. Since the number of breakings off and rejoinings grows only logarithmically with the ratio of the loop size to the curvature radius at the kink, and since the entire phenomenon is quite rare, we do not expect it to have any observable consequences.

---

[1] A. Vilenkin and E.P.S. Shellard, *Cosmic Strings and Other Topological Defects*, Cambridge University Press, Cambridge, England, (1994).

[2] E. Witten, "Cosmic Superstrings," Phys. Lett. **B153**, 243 (1985).

[3] S. Sarangi and S.-H. H. Tye, "Cosmic string production towards the end of brane inflation," Phys. Lett. B **536**, 185 (2002)

[4] G. Dvali and A. Vilenkin, "Formation and evolution of cosmic D-strings," JCAP **0403**, 010 (2004).

[5] E. J. Copeland, R. C. Myers and J. Polchinski, "Cosmic F- and D-strings," JHEP **0406**, 013 (2004).

[6] N. Kaiser and A. Stebbins, "Microwave Anisotropy Due To Cosmic Strings," Nature **310**, 391 (1984).

[7] A. Vilenkin, "Cosmic Strings As Gravitational Lenses," Astrophys. J. **282**, L51 (1984); J. R. I. Gott, "Gravitational lensing effects of vacuum strings: Exact solutions," Astrophys. J. **288**, 422 (1985); A. Vilenkin, "Looking For Cosmic Strings," Nature (London), **322**, 613 (1986); B. Shlaer and S.-H. H. Tye, "Cosmic string lensing and closed time-like curves," Phys. Rev. D **72**, 043532 (2005).

[8] M. Wyman, L. Pogosian and I. Wasserman, "Bounds on cosmic strings from WMAP and SDSS," Phys. Rev. D **72**, 023513 (2005) [Erratum-ibid. D **73**, 089905 (2006)]; A. A. Fraisse, "Limits on Defects Formation and Hybrid Inflationary Models with Three-Year WMAP Observations," JCAP **0703**, 008 (2007).

[9] N. Bevis, M. Hindmarsh, M. Kunz and J. Urrestilla, "CMB power spectrum contribution from cosmic strings using field-evolution simulations of the Abelian Higgs model," Phys. Rev. D **75**, 065015 (2007); N. Bevis, M. Hindmarsh, M. Kunz and J. Urrestilla, "Fitting CMB data with

cosmic strings and inflation," Phys. Rev. Lett. **100**, 021301 (2008); J. Urrestilla, N. Bevis, M. Hindmarsh, M. Kunz and A. R. Liddle, "Cosmic microwave anisotropies from BPS semilocal strings," JCAP **0807**, 010 (2008); P. Mukherjee, J. Urrestilla, M. Kunz, A. R. Liddle, N. Bevis and M. Hindmarsh, "Detecting and distinguishing topological defects in future data from the CMBPol satellite," Phys. Rev. D **83**, 043003 (2011).

[10] N. Bevis, M. Hindmarsh, M. Kunz and J. Urrestilla, "CMB power spectra from cosmic strings: predictions for the Planck satellite and beyond," Phys. Rev. D **82**, 065004 (2010).

[11] A. Vilenkin, "Gravitational Radiation From Cosmic Strings," Phys. Lett. B **107**, 47 (1981); T. Vachaspati and A. Vilenkin, "Gravitational Radiation From Cosmic Strings," Phys. Rev. D **31**, 3052 (1985); C. J. Burden, "Gravitational Radiation From A Particular Class Of Cosmic Strings," Phys. Lett. B **164**, 277 (1985); D. Garfinkle and T. Vachaspati, "Radiation from kinky, cuspless cosmic loops," Phys. Rev. D **36**, 2229 (1987).

[12] T. Damour and A. Vilenkin, "Gravitational wave bursts from cosmic strings," Phys. Rev. Lett. **85**, 3761 (2000); T. Damour and A. Vilenkin, "Gravitational wave bursts from cusps and kinks on cosmic strings," Phys. Rev. D **64**, 064008 (2001); X. Siemens, J. Creighton, I. Maor, S. Ray Majumder, K. Cannon and J. Read, "Gravitational wave bursts from cosmic (super)strings: Quantitative analysis and constraints," Phys. Rev. D **73**, 105001 (2006); C. J. Hogan, "Gravitational waves from light cosmic strings: Backgrounds and bursts with large loops," Phys. Rev. D **74**, 043526 (2006); S. Olmez, V. Mandic and X. Siemens, "Gravitational-Wave Stochastic Background from Kinks and Cusps on Cosmic Strings," Phys. Rev. D **81**, 104028 (2010).

[13] T. Vachaspati, A. E. Everett and A. Vilenkin, "Radiation From Vacuum Strings And Domain Walls," Phys. Rev. D **30**, 2046 (1984); R. H. Brandenberger, "On the decay of cosmic string loops," Nucl. Phys. B **293**, 812 (1987); M. Mohazzab, "Cusp annihilation on ordinary cosmic strings," Int. J. Mod. Phys. D **3**, 493 (1994); J. J. Blanco-Pillado and K. D. Olum, "The form of cosmic string cusps," Phys. Rev. D **59**, 063508 (1999); K. D. Olum and J. J. Blanco-Pillado, "Field theory simulation of Abelian-Higgs cosmic string cusps," Phys. Rev. D **60**, 023503 (1999).

[14] G. Vincent, N. D. Antunes and M. Hindmarsh, "Numerical simulations of string networks in the Abelian-Higgs model," Phys. Rev. Lett. **80**, 2277 (1998).

[15] K. D. Olum and J. J. Blanco-Pillado, "Radiation from cosmic string standing waves," Phys. Rev. Lett. **84**, 4288 (2000).

[16] J. N. Moore, E. P. S. Shellard and C. J. A. Martins, "On the evolution of Abelian-Higgs string networks," Phys. Rev. D **65**, 023503 (2001).

[17] R. L. Davis, "Cosmic Axions from Cosmic Strings," Phys. Lett. B **180**, 225 (1986); A. Vilenkin and T. Vachaspati, "Radiation of Goldstone bosons from cosmic strings," Phys. Rev. D **35**, 1138 (1987); R. L. Davis and E. P. S. Shellard, "Do Axions Need Inflation?," Nucl. Phys. B **324**, 167 (1989); R. A. Battye and E. P. S. Shellard, "Global string radiation," Nucl. Phys. B **423**, 260 (1994).

[18] T. Damour and A. Vilenkin, "Cosmic strings and the string dilaton," Phys. Rev. Lett. **78**, 2288 (1997); E. Babichev and M. Kachelriess, "Constraining cosmic superstrings with dilaton emission," Phys. Lett. B **614**, 1 (2005);

[19] M. Srednicki and S. Theisen, "Nongravitational Decay Of Cosmic Strings," Phys. Lett. B **189**, 397 (1987); M. Peloso and L. Sorbo, "Moduli from cosmic strings," Nucl. Phys. B **649**, 88 (2003); E. Sabancilar, "Cosmological Constraints on Strongly Coupled Moduli from Cosmic Strings," Phys. Rev. D **81**, 123502 (2010); T. Vachaspati, "Cosmic Rays from Cosmic Strings with Condensates," Phys. Rev. D **81**, 043531 (2010); D. A. Steer and T. Vachaspati, "Light

from Cosmic Strings," arXiv:1012.1998 [hep-th].

[20] V. Berezinsky, P. Blasi and A. Vilenkin, "Ultra high energy gamma rays as signature of topological defects," Phys. Rev. D **58**, 103515 (1998); P. Bhattacharjee and G. Sigl, "Origin and propagation of extremely high energy cosmic rays," Phys. Rept. **327**, 109 (2000).

[21] A. Vilenkin, "Cosmological Density Fluctuations Produced by Vacuum Strings," Phys. Rev. Lett. **46**, 1169-1172 (1981).

[22] T. W. B. Kibble, "Evolution Of A System Of Cosmic Strings," Nucl. Phys. **B252**, 227 (1985).

[23] D. P. Bennett, "The Evolution Of Cosmic Strings," Phys. Rev. **D33**, 872 (1986); D. P. Bennett, "Evolution Of Cosmic Strings. 2.," Phys. Rev. **D34**, 3592 (1986).

[24] A. Albrecht and N. Turok, "Evolution Of Cosmic Strings," Phys. Rev. Lett. **54**, 1868 (1985).

[25] A. Albrecht and N. Turok, "Evolution Of Cosmic String Networks," Phys. Rev. D **40**, 973 (1989).

[26] D. P. Bennett and F. R. Bouchet, "Evidence For A Scaling Solution In Cosmic String Evolution," Phys. Rev. Lett. **60**, 257 (1988); D. P. Bennett and F. R. Bouchet, " Cosmic string evolution," Phys. Rev. Lett. **63**, 2776 (1989).

[27] D. P. Bennett and F. R. Bouchet, "High resolution simulations of cosmic string evolution. 1 Network evolution," Phys. Rev. D **41**, 2408 (1990).

[28] B. Allen and E. P. S. Shellard, "Cosmic string evolution: A numerical simulation," Phys. Rev. Lett. **64**, 119 (1990).

[29] D. Austin, E. J. Copeland and T. W. B. Kibble, "Evolution Of Cosmic String Configurations," Phys. Rev. D **48**, 5594 (1993).

[30] C. J. A. P. Martins, E. P. S. Shellard, "Quantitative string evolution," Phys. Rev. **D54**, 2535-2556 (1996).

[31] J. Polchinski and J. V. Rocha, "Analytic Study of Small Scale Structure on Cosmic Strings," Phys. Rev. D **74**, 083504 (2006); J. Polchinski and J. V. Rocha, "Cosmic string structure at the gravitational radiation scale," Phys. Rev. D **75**, 123503 (2007). F. Dubath, J. Polchinski and J. V. Rocha, "Cosmic String Loops, Large and Small," Phys. Rev. D **77**, 123528 (2008);

[32] V. Vanchurin, K. Olum and A. Vilenkin, "Cosmic string scaling in flat space," Phys. Rev. D **72**, 063514 (2005).

[33] C. Ringeval, M. Sakellariadou and F. Bouchet, "Cosmological evolution of cosmic string loops," JCAP **0702**, 023 (2007).

[34] C. J. A. P. Martins and E. P. S. Shellard, "Fractal properties and small-scale structure of cosmic string networks," Phys. Rev. D **73**, 043515 (2006).

[35] V. Vanchurin, K. D. Olum and A. Vilenkin, "Scaling of cosmic string loops," Phys. Rev. D **74**, 063527 (2006).

[36] K. D. Olum, V. Vanchurin, "Cosmic string loops in the expanding Universe," Phys. Rev. **D75**, 063521 (2007).

[37] J. J. Blanco-Pillado, K. D. Olum and B. Shlaer, "A new parallel simulation technique," arXiv:1011.4046 [physics.comp-ph].

[38] V. Vanchurin, "Non-linear dynamics of cosmic strings with non-scaling loops," Phys. Rev. **D82**, 063503 (2010); V. Vanchurin, "Semi-scaling cosmic strings," JCAP **1011**, 013 (2010).

[39] T. Vachaspati and A. Vilenkin, "Formation And Evolution Of Cosmic Strings," Phys. Rev. D **30**, 2036 (1984).

[40] "Scaling distribution of large cosmic string loops," Talk presented by K. D. Olum at the conference, "Challenges in Theoretical Cosmology", Talloires, France, (2009).

[41] J. J. Blanco-Pillado, K. D. Olum and B. Shlaer, in preparation.

[42] F. Bouchet, "High-resolution Simulations of Cosmic String Evolution: Small Scale Structure and Loops" in *The formation and evolution of cosmic strings*, G. Gibbons, S. Hawking, and T. Vachaspati, eds., Cambridge University Press, Cambridge, England, (1990).